This is a repository copy of *The transcriptional landscape of the cultured murine middle ear epithelium in vitro*.

White Rose Research Online URL for this paper:
https://eprints.whiterose.ac.uk/173574/

Version: Published Version

Article:

The Company of Biologists

RESEARCH ARTICLE

The transcriptional landscape of the cultured murine middle ear epithelium *in vitro*

Apoorva Mulay[1], Md Miraj K. Chowdhury[1], Cameron T. James[1], Lynne Bingle[2] and Colin D. Bingle[1,3,*]

ABSTRACT

Otitis media (OM) is the most common paediatric disease and leads to significant morbidity. Although understanding of underlying disease mechanisms is hampered by complex pathophysiology, it is clear that epithelial abnormalities underpin the disease. The mechanisms underpinning epithelial remodelling in OM remain unclear. We recently described a novel *in vitro* model of mouse middle ear epithelial cells (mMEECs) that undergoes mucociliary differentiation into the varied epithelial cell populations seen in the middle ear cavity. We now describe genome wide gene expression profiles of mMEECs as they undergo differentiation. We compared the gene expression profiles of original (uncultured) middle ear cells, confluent cultures of undifferentiated cells and cells that had been differentiated for 7 days at an air liquid interface (ALI). >5000 genes were differentially expressed among the three groups of cells. Approximately 4000 genes were differentially expressed between the original cells and day 0 of ALI culture. The original cell population was shown to contain a mix of cell types, including contaminating inflammatory cells that were lost on culture. Approximately 500 genes were upregulated during ALI induced differentiation. These included some secretory genes and some enzymes but most were associated with the process of ciliogenesis. The data suggest that the *in vitro* model of differentiated murine middle ear epithelium exhibits a transcriptional profile consistent with the mucociliary epithelium seen within the middle ear. Knowledge of the transcriptional landscape of this epithelium will provide a basis for understanding the phenotypic changes seen in murine models of OM.

KEY WORDS: *In vitro*, Middle ear, Otitis media, Transcriptomics

INTRODUCTION

Otitis media (OM), a group of inflammatory diseases of the middle ear, is the leading cause of paediatric surgery and the most frequent reason for the prescription of antibiotics (Bakaletz, 2010; Woodfield and Dugdale, 2008). It can have both acute and chronic (recurrent) presentations the consequences of which may be life-long. Over 80% of children develop at least one incidence of OM by 3 years of age and over 700 million cases occur world-wide per year (Monasta et al., 2012).

[1]Department of Infection, Immunity and Cardiovascular Disease, University of Sheffield, Sheffield S10 2RX, UK. [2]Oral and Maxillofacial Pathology, Department of Clinical Dentistry, University of Sheffield, Sheffield S10 2TA, UK. [3]The Florey Institute for Host Pathogen Interactions, University of Sheffield, Sheffield S10 2TN, UK.

*Author for correspondence (c.d.bingle@sheffield.ac.uk)

L.B., 0000-0002-4587-9384; C.D.B., 0000-0002-5405-6988

Children with recurrent episodes of OM are at risk of developing hearing loss and it is estimated that, globally, over 100 million people have hearing loss due to OM. Consequently, the disease is a major paediatric clinical problem that produces significant morbidity and quality-of-life issues across the world, with the major burden being seen in children in developing countries (Monasta et al., 2012).

The middle ear epithelium and its secretions are involved in maintaining homeostasis and sterility within the middle ear cavity (MEC). Multiple host defence proteins have been shown to help protect the middle ear cavity. For example, we recently identified BPIFA1 as an abundant secretory protein produced by the middle ear epithelium and showed that loss of the gene exacerbated disease severity in an established model of OM (Mulay et al., 2018). Furthermore, loss of the gel forming mucin, MUC5B has also been shown to cause OM (Roy et al., 2014). OM can be considered to be a disease of the middle ear epithelium. The epithelial lining of the middle ear cavity varies according to the location (Luo et al., 2017; Tucker et al., 2018). The epitympanum is lined by squamous epithelium while the middle ear proper is lined by cuboidal epithelium and the hypotympanum by ciliated columnar epithelium. Phenotypic changes throughout the middle ear epithelium are key to the pathophysiology of OM (Tucker et al., 2018; Thompson and Tucker, 2013). Current knowledge suggests that OM is caused by an unrestrained response by the middle ear epithelium to an exogenous trigger, often a pathogen (Juhn et al., 2008; Kurabi et al., 2016). This is associated with excess production of secretory proteins from the abnormal epithelium, which along with an important contribution of inflammatory cells, produce middle ear exudates (Bakaletz, 2010). The mechanisms underpinning the epithelial remodelling remain unclear but a complex interaction between the epithelium, unrestrained inflammatory cells and otopathogens, results in the development of an abnormal mucociliary epithelium that contributes to the development of the characteristic exudates.

The ability to identify the function of different epithelial cell types and their products within the middle ear has limited our understanding of phenotypic changes underpinning OM development. Research into the pathogenesis of OM is limited because of difficulties in accessing appropriate samples, at an early stage in the disease process. Most studies have involved sampling the middle ear fluid (Preciado et al., 2010) or been restricted to whole animal challenge studies (Preciado et al., 2013; Davidoss et al., 2018; Del-Pozo et al., 2019; Hernandez et al., 2015; MacArthur et al., 2013) We recently described the establishment of an air liquid interface (ALI) culture system to model the mouse middle ear epithelium *in vitro* (Mulay et al., 2016, 2019). We showed that a 'basal cell-like' population of middle ear epithelial cells underwent differentiation during ALI culture to generate a complex mucosal tissue that had characteristics of the native middle ear epithelium (Mulay et al., 2016, 2019). We could also show that these cells were readily infected by the otopathogen, non-typeable *Haemophilus influenzae* (Mulay et al., 2016), confirming their potential utility as a model for infection studies. We now describe

genome-wide gene expression profiles of these cells as they undergo differentiation to provide an understanding of the transcriptional landscape of this complex epithelium when grown *in vitro*.

RESULTS

We previously showed that mouse middle ear epithelial cells (mMEECs) undergo a process of mucociliary differentiation over a period of 14 days when cultured at the ALI. In this study we used cells that were isolated from mouse bullae and cultured for 7 days at the ALI (shown schematically in Fig. 1A). We used end point PCR to confirm that the cells switched on genes associated with differentiated secretory (*Bpifa1*) and ciliated cells (*Tekt1*) within 3 days of establishment of ALI culture (Fig. 1B). We then used gene expression array analysis to compare the gene expression profiles of matched, triplicate samples of original (uncultured) middle ear cells, confluent cultures of undifferentiated cells (day 0 of ALI) and cells that had been differentiated for 7 days at the ALI (Table 1). The original cells used to initiate the cultures would be expected to contain a mixture of cells including different epithelial cells along with inflammatory and blood cells recovered from the tissue during isolation.

Principal Component Analysis (Fig. 2A) showed that the three different sample groups were clustered together, although the original cell sample exhibited the greatest variability. The 20 most highly expressed at each time point are listed in Table 1. In the original cells four of these genes represented haemoglobin genes and the three top

secretory protein gene were *Bpifa1*, *Lyz2* and *Bpifb1*. At day 0 of culture all but one of the top 20 genes were structural, with the exception of *Lcn2*. By day 7 of ALI culture the most highly expressed genes included multiple secretory protein genes including, *Lcn2*, *Reg3g*, *Bpifa1*, *Cp*, *Ltf* and *Tf*. This expression data is in keeping with our previous proteomic data that identified these as being amongst the most abundant proteins in apical secretions from ALI cells (Table 1) (Mulay et al., 2016). Other highly expressed genes are not necessarily associated with epithelial cell specific function but rather are probably highly expressed in multiple cell types and may be considered to encode protein with 'house-keeping' functions.

Following Robust MuitiArray Average (RMA) normalisation (Phipson et al., 2016) differential gene expression was undertaken using Limma (Smyth, 2004) This analysis (Fig. 2B) revealed that a total of 5261 genes were differentially expressed amongst the three different groups with an absolute fold change of >2 and a Limma adjusted P-value of <0.05. The heat map clearly shows that samples from the different time points group together but also shows some level of variability between individual samples. When comparing different time points 1580 genes were significantly more highly expressed in the original cells compared to the day 0 cultures whereas 2400 genes were more highly expressed in the day 0 cells compared to the original cells (Table S1). The most highly differentially expressed genes in the original samples were, *Lipf*, *Hbb-bs*, *Hbb-bt*, *Bpifb1* and *Lyz1*, whereas in the day 0 cells they were *Arg1*, *Sorbs2*,
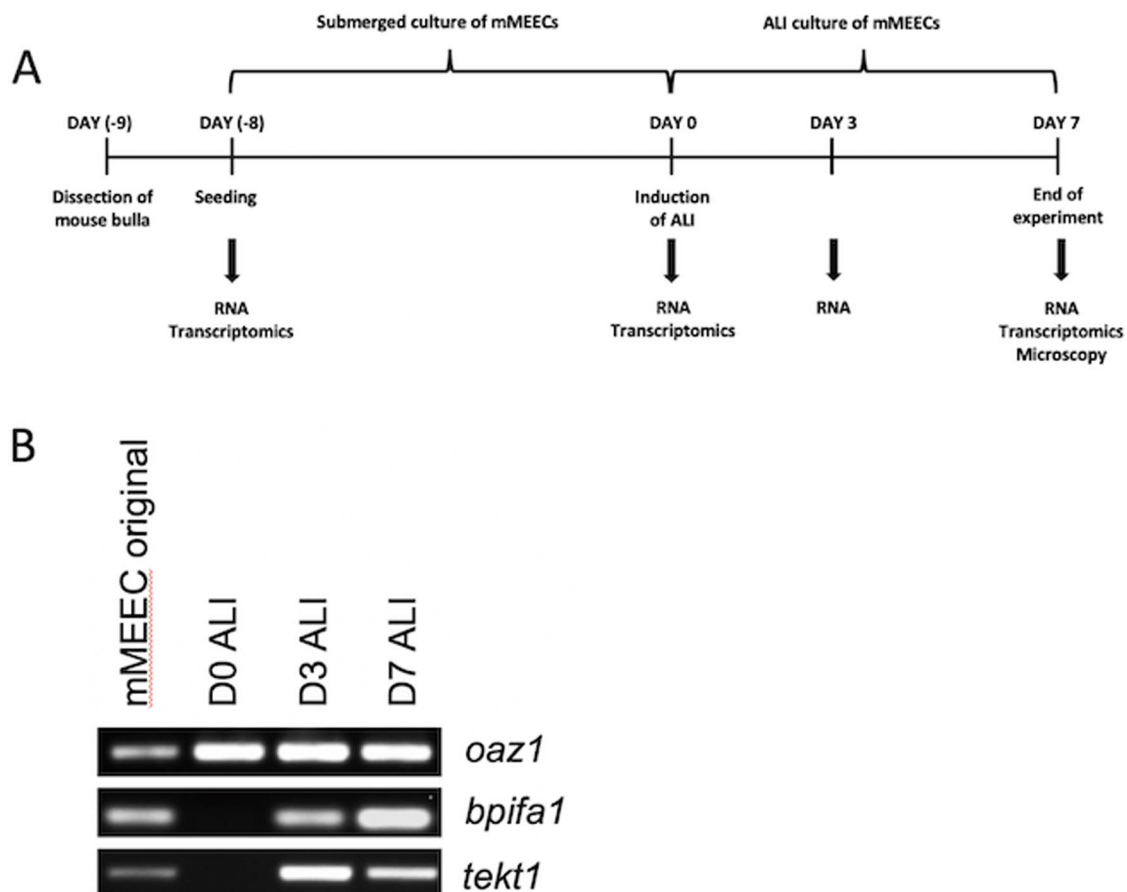
Fig. 1. Culture of mMEECs for transcriptional analysis. (A) Schematic timeline for culture experiments. mMEECs were isolated from dissected bullae (day −9) and cultured in transwells in submerged culture until confluence (day −8 to day 0), before ALI was induced. Samples for transcriptional analysis were collected at seeding (original cells), day 0, day 3 and day 7. (B) End-point RT-PCR showing expression of *Oaz1*, *Bpifa1* and *Tekt1* in mMEEC original cells isolated from the middle ear cavity, ALI day 0, 3 and 7 cells. This is a representative sample.

Table 1. The top 20 genes from each set of samples are listed in descending level of expression. Data was log transformed. The presumptive function of each gene is also outlined. The proteome column shows the ranking of each secreted protein in the day 15 secreted proteome of ALI mMEECs cells taken from Mulay *et al*, 2016.

			Day 0			Day 7			
Gene Symbol	Avg (log2)	Function	Gene Symbol	Avg (log2)	Function	Gene Symbol	Avg (log2)	Function	Proteome
Hba-a1; Hba-a2	18.84	Oxygen transport	Lcn2	19.58	Iron sequestration	Lcn2	19.58	Iron sequestration	4th
Hba-a2; Hba-a1	18.84	Oxygen transport	Clu	19.44	Chaperone	Clu	19.49	Chaperone	
Bpifa1	18.81	Host defence	Ly6e	19.38	TCR signalling	Ly6e	19.39	TCR signalling	
Lyz2	18.81	Antibacterial	Cd81	19	Tetraspanin	Reg3g	19.37	Antibacterial	3rd
Cldn4	18.81	Tight Junction	Bsg	18.85	Immunoglobulin superfamily	Cyp2f2	19.31	Metabolism	
Bpifb1	18.81	Host defence	Ly6a	18.82	Lipd raft signalling	Bpifa1	19.24	Host defence	7th
Dmbt1	18.77	Scavenger receptor	Eno1; Eno1b	18.79	Gycolysis	Cp	19.17	Metal transport	5th
Hbb-bs; Hbb-b1	18.77	Oxygen transport	Mt1	18.77	Metal binding	Cbr2	19.03	Carbonyl metabolism	
Eif1	18.71	Translation	Sprr2a2; Sprr2a1	18.75	Barrier functionn	Ltf	18.92	Metal transport	1st
Lipf	18.67	Lipase	Cbr2	18.63	Carbonyl metabolism	Tmem176b	18.79	Dendritic cells	
Hbb-bt; Hbb-b2	18.67	Oxygen transport	Serinc3	18.51	Viral Restriction	Trf	18.78	Metal transport	2nd
Rmrp	18.65	Ribonuclease	Itm2b	18.5	Amyloid binding	Gsto1	18.63	Glutathione transferase	
Tmsb4x	18.62	Actin			polymerisationn	Tmsb4x	18.47	Actin polymerisationn	
Ly6a	18.62	Lipid raft signalling							
Dusp1	18.57	Phosphatase	Dad1	18.41	Glycosylation	Serinc3	18.61	Viral restriction	
Mt1	18.55	Metal binding	Mt2	18.35	Metal binding	Gstm1	18.58	Glutathione transferase	
Cyr61	18.43	ECM signalling	Igfbp7	18.27	IGF regulation	Bsg	18.51	Immunoglobulin superfamily	
Mt2	18.33	Metal binding	Gsto1	18.23	Glutathione transferase	Dad1	18.5	Glycosylation	
Wfdc18	18.19	Protease inhibitor	Rps6	18.22	Ribosome	Itm2b	18.48	Amyloid binding	
Ly6e	18.17	TCR signalling	Rpl12; Snora65	18.2	Ribosome	Lyz2	18.36	Antibacterial	22nd
Slc3a2	18.17	Transporter	Rpl28	18.14	Ribosome	Cd81	18.27	Tetraspanin	

Srd5a1, *Vsnl1* and *Lox*. When day 0 cells were compared to day 7 ALI cells many fewer genes were differentially expressed. 489 genes were upregulated as the cells differentiated whereas expression of 385 genes were significantly reduced (Table S2). The most highly differentially expressed genes in the day 7 samples were, *Lyz2*, *Aldh1a1*, *Spata18*, *Cdhr3* and *Lrrc34*, whereas in the day 0 cells they were *Ppbp (Cxcl7)*, *Lgals1 (Galectin1)*, *Il1a*, *Ndufa412* and *2610528A11Rik (Gpr15l)*. Comparisons between the original cells and the day 7 ALI cells showed that 2408 genes were upregulated whereas 1215 genes were downregulated (Table S3). The most highly differentially expressed genes in the day 7 samples were, *Fetub*, *Sorbs2*, *Rgs5*, *Serpina7* and *Kcnj16*, whereas in the original cells they were *Lipf*, *Bpifb1*, *Hbb-bs*, *Hbb-bt*, and *Hba-a2*.

To gain more information from the differential gene expression data sets we subjected them to gene ontology analysis using clusterProfiler (Yu et al., 2012). For this analysis we were most interested in understanding the processes that occurred as epithelial cells became confluent during the submerged culture period and what happened when the cells underwent differentiation. With this in mind we focused our analysis on identifying genes upregulated as the cells became confluent and also on those that were upregulated

as the cells differentiated. The top biological processes enriched as the cells reached confluence at day 0 included those associated with cell division, cell migration and cell activation (Fig. 2C). In the day 7 cells the majority of pathways identified were associated with aspects of ciliogenesis or ciliary function (Fig. 2D). Close inspection of the differential gene list from this time point allowed the identification of many genes that are shown to be associated with cilia, including *Spata18*, *Cdhr3*, *Lrrc34*, *Dynlrb2*, *Lrguk*, *Dnah6*, *Ccdc67*, *Dhrs9*, *Spef2*, and *ccdc146*. *Tekt1* the gene we use as a ciliated cell specific marker in our end-point PCR reactions was the twenty-sixth most differentially expressed in this list (Table S2). We used end-point PCR with RNA extracted from a different batch of cells to confirm that *Spata18*, *Cdhr3* and *dynlrb2* were upregulated during the process of differentiation (Fig. 2E).

Expression of OM associated genes in the *in vitro* mouse middle ear epithelium

One of the potential uses of our *in vitro* model, is that it may be useful for the study of genes associated with OM. Multiple genetic association studies have been undertaken to identify human genes associated with OM (Allen et al., 2013; Rye et al., 2012; Einarsdottir
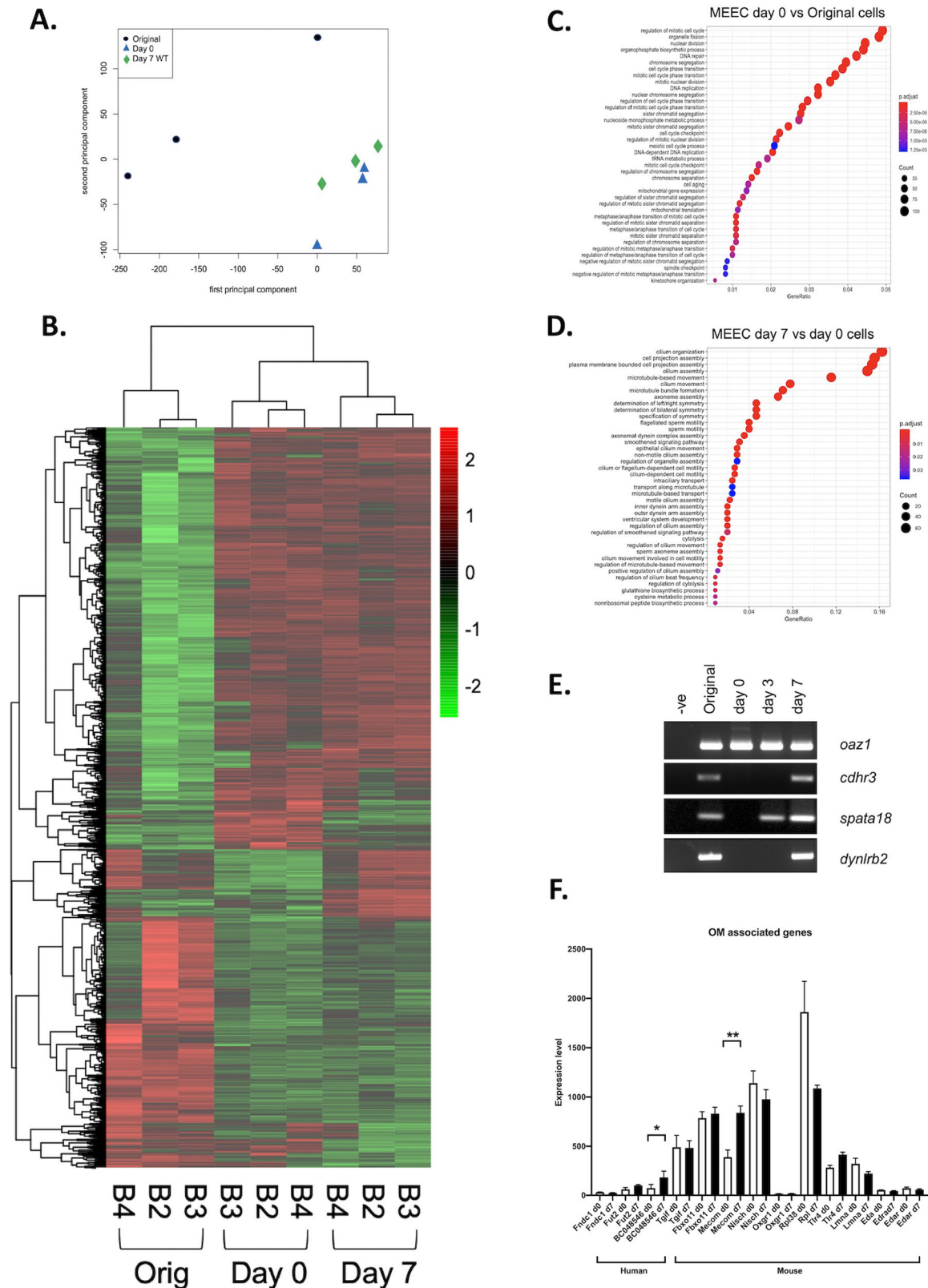
Fig. 2. Genome wide transcriptional analysis of differentiating mMEECs. (A) PCA analysis was used to show the relatedness of the different samples used in the study. (B) The heatmap shows differentially expressed genes identified by Limma. Genes used in the analysis were >2-fold differentially expressed. (C,D) Gene ontogeny analysis of the most highly differentially expressed genes are displayed for day 0 versus original cells (C) and day 7 versus day 0 (D). (E) A representative end-point RT-PCR showing expression of *Oaz1*, *Cdhr3*, *Spata18* and *Dynlrb2* in cDNA from mMEEC original cells isolated from the middle ear cavity, ALI day 0, 3 and 7 cells. Negative control samples contained no cDNA. (F) Microarray derived data of relative expression of candidate OM associated genes in day 0 and day 7 cells. *P >0.05; **P >0.01 using log transformed data. Human and mouse candidate genes are identified.

et al., 2016; Giese et al., 2020). Additionally, loss of function of multiple genes have been shown to lead to the development of OM-like phenotypes in mice (Rye et al., 2011; Bhutta et al., 2017). Expression of three well validate human OM associated genes *Fndc1* (van Ingen et al., 2016), *Fut2* (Santos-Cortez et al., 2018) and *A2ml1* (*BC048546*) (Santos-Cortez et al., 2015) was detected in the mMEECs with the highest expression being for *BC048546* in the day 7 differentiated cells (Fig. 2F). Expression of four OM associated genes identified through ENU mutagenesis screening: *Tgif1* (Tateossian et al., 2013), *Fxbxo11* (Hardisty-Hughes et al., 2006), *Mecom* (Parkinson et al., 2006) and *Nisch* (Crompton et al., 2017) is clearly seen in both the undifferentiated and differentiated cells, with *Mecom* (*Evi1*), the gene mutated in the *Junbo*$^{+/-}$ OM mouse model (Mulay et al., 2018; Parkinson et al., 2006), being most differentially expressed during differentiation. The expression of a further, representative group of genes associated with murine OM was shown to be variable with *Oxgr1* (Kerschner et al., 2013) being essentially not expressed in the cells whereas *Rpl38* (Noben-Trauth and Latoche, 2011) was the most highly expressed (data not shown). This simple analysis shows that, although there was not clear differentiation associated changes in many of these genes, this data set will be useful to understand something about the epithelial expression of OM candidate genes.

DISCUSSION

The mucosal lining of the middle ear cavity covers the entire surface and varies according to the location (Luo et al., 2017; Tucker et al., 2018). Cellular morphology can be simple squamous, cuboidal or columnar depending on the location and can have tracts of ciliated cells interspersed with secretory cells. We recently described a method to differentiate primary mMEECs at an air liquid interface. We could show that the differentiated cultures took on a morphology similar to that seen *in situ*, with tracts of elevated columnar mucociliary epithelium that contained both ciliated (FOXJ1^{+ve}) and goblet (MUC5B^{+ve}) cells alongside cuboidal (BPIFA1^{+ve}) cells (Mulay et al., 2016). This model system overcomes a major limitation of previous middle ear epithelial cultures, namely the lack of differentiation into distinct epithelial cell types that are hallmarks of the mucociliary epithelium seen in the murine middle ear.

In this study we have used an unbiased expression array approach to better define the transcriptional signature of this *in vitro* murine middle ear epithelial model. We chose to study a single time point of 7 days of differentiation so as to capture the development of early stages of the mucociliary differentiation that occurs in this model. The transcriptional differences in the cultures at the three different times points were striking. The original cells, a cell population that had been depleted of fibroblasts (perhaps not completely, as judged by expression of *Col1a1* and *Col1a2* in the samples) by a differential adherence step, were made up of a mixture of cells from the middle ear. In this cell population *Bpifa1* was the most highly expressed secretory gene. Unsurprisingly, this population of cells exhibited a strong differential gene expression signature for myeloid cells, including macrophages and neutrophils, represented by *S100a8*, *Ngp*, *Lilrb4a*, *Retnlg* and *Spi1*. Amongst the other highly expressed genes in the original cells were multiple haemoglobin genes, potentially indicating that some blood contaminated the isolated cells. However, Hb genes have been shown to be expressed in multiple cells as well as in erythrocyte precursors (Biagioli et al., 2009; Bhaskaran et al., 2005; Stamatoyannopoulos, 2005). There was also very high differential expression of *Lyz1* and *Lyz2* both of which are known to be expressed in both macrophages and structural lung cells (Cross et al., 1988; Montoro et al., 2018). The list also included some

unexpected genes. For example, the top differentially expressed gene was gastric lipase (*Lipf*), a gene that has not previously shown to be expressed in the ear, but that has been shown to be expressed in goblet cells of the airways (Montoro et al., 2018). Consistent with our previous data (Mulay et al., 2016), we could show that *Bpifb1* was highly expressed in the original cell population but that expression was lost in the day 0 cells. Expression of this gene did not recover to the levels of the original after 7 days of differentiation. BPIFB1 is a marker of a population of goblet cells in the upper respiratory tract and nasopharynx of mice (Musa et al., 2012) and is present in human COME exudates (Preciado et al., 2010). Consistent with the gene expression data we did not detect BPIFB1 in apical secretions from mMEECs (Mulay et al., 2016). We assume that perhaps the *Bpifb1* signal comes from a 'goblet' cell population that is not cultured in our system. Other goblet cell markers, including *Tff2* and *Muc5B* (Montoro et al., 2018) (but not the other gel forming mucin gene, *Muc5AC*) also exhibited a similar expression pattern. It is possible that these cells may emanate from the eustachian tube.

During the 7-day period when the cells were grown at the ALI the most striking signature seen across differentially expressed genes was one of cilia and ciliogenesis. Amongst the top differentially expressed genes were also some secretory protein genes. This observation confirms that the cultured cells underwent mucociliary differentiation. This gene signature is consistent with our previous IF studies that showed the presence of ciliated, secretory and basal cells in the cultures (Mulay et al., 2016). These *in vitro* data are also consistent with *in vivo* studies that have shown the presence of cuboidal epithelial cells expressing secretory proteins alongside regions of ciliated cells (Luo et al., 2017; Tucker et al., 2018). Although some of the ciliated cell signature genes are reasonably well studied such as, *Spata18* (Bornstein et al., 2011) and *Cdhr3* (Everman et al., 2019), only *Dynlrb2* has been identified in the ear (Ryan et al., 2020). The process multiciliogenesis is very complex and involves the concerted action of multiple pathways that regulate hundreds of genes that together make up the ciliary architecture (Choksi et al., 2014). It may be that some aspects of multiciliogenesis in this location involve unique genes. It will be interesting to apply comparative analysis with data from other murine multiciliated tissues to see if such unique genes exist.

One of the limitations of this study is that is provides bulk gene expression data from the epithelial model in total. It does not provide any cell specific gene expression information. However, the data presented here do complement the recent scRNAseq data generated from murine middle ear mucosa *in vivo* (Ryan et al., 2020). Sequencing of single cell suspensions isolated from middle ear mucosa overlying the bullar bone identified seventeen distinct cells types on the basis of transcriptional signatures. Five of these (representing over 50% of total cells recovered) were designated as epithelial cells. One expressing *Dynlrb2* represented ciliated cells, one expressing *Krt14* represented basal cells, and three represented some type of secretory cells. These appeared to be closely related and expressed relatively few genes exclusively. The analysis did not identify a goblet cell population mirroring what we see in our data. Further analysis of the data might allow for a subdivision of epithelial cell types as has been reported in the murine trachea (Montoro et al., 2018; Chu et al., 2019) and nasal passages (Ziegler et al., 2020). Alternatively, the epithelial cell population may well differ between geographical location. It will be important to address this cell specificity in the future.

Multiple mouse models are available for the study of OM. These include mice deficient in genes such as *Tgif1*, *Mecom*/*Evi1*, *Fbxo11*, *Tlr4*, *Eda* and *Edar* (Tateossian et al., 2013; Hardisty-Hughes et al., 2006; Parkinson et al., 2006; Crompton et al., 2017; Kerschner et al.,

2013; MacArthur et al., 2006; Azar et al., 2016). These genes are all expressed in the ALI cultures, although not all of them show expression associated with differentiation. *Mecom/Evi1* is the gene that appears to show the largest difference between the differentiated and undifferentiated cultures. We have recently shown that the *Junbo*$^{-/+}$ OM mouse, which is heterozygous for a mutation in *Mecom/Evi1* (Parkinson et al., 2006), develops an exacerbated OM phenotype when *Bpifa1* is also removed (Mulay et al., 2018). In addition, the ALI cultured cells also exhibit expression of some known human OM susceptibility genes. Most interestingly, the differentiated cells strongly express *BC048546*, a presumptive orthologue of *A2ML1*, a well validated human OM susceptibility gene, which is present in the murine middle ear (Santos-Cortez et al., 2015). Our data suggests that the differentiated mMEEC culture system might have utility for reproducing the OM phenotype of these mouse mutants *in vitro* and enable comparative studies between unaffected and diseased cultures. Our data can also be used to understand the expression and localisation of other disease-causing mutations, for example in genes associated with primary ciliary dyskinesia, an autosomal recessive genetic disorder that causes defects in the action of cilia and can result in OM (Mata et al., 2014). Ultimately, it will be interesting to compare our data with that seen in human middle ear cells cultured in a similar manner (Chen et al., 2019).

Although our data provides a transcriptional signature of the murine middle ear epithelium as it undergoes the process of mucociliary differentiation *in vitro*, it is missing any protein data. We recognise that it is proteins that drive cellular processes such a differentiation and generating a proteomic signature of this process is important as gene expression is not always correlated with protein translation (Edfors et al., 2016). Our previous proteomic analysis of apical secretions from similar cultures did identify many of the genes we identified in of expression data set (Mulay et al., 2016).

In conclusion, we have presented data describing the gene expression changes in primary murine middle ear cells as they become differentiated when cultured at an ALI. Consistent with our established understanding of the cellular composition of the middle ear this signature describes a mucociliary epithelium. This data set provides a complete transcriptome of the *in vitro* middle ear epithelium when cultured in a manner than encourages differentiation. This will be a valuable tool for understanding the role played by candidate genes in the middle ear and during the development of OM.

MATERIALS AND METHODS
Ethics statement
All animal experiments were performed at the University of Sheffield in accordance with the UK Animals (Scientific procedures) Act, authorized under a UK Home Office License (project license number is P4802B8AC) and approved by the animal project review committee of the University of Sheffield. 8–10-week-old C57BL6 mice of mixed sex were used in this study. Mice were housed in ventilated cages under specific pathogen free conditions. Mice were euthanised by overdose of pentobarbitone followed by exsanguination.

Isolation and differentiation of middle ear epithelial cells at air liquid interface
The protocol for primary culture and differentiation of mMEECs has been described in detail previously (Mulay et al., 2016, 2019). Five or six mice of mixed sexes (10–12 bullae) were used for each cell isolation. Following a differential adherence step that removes contaminating fibroblasts, the original cell population contains a mix of cell types including differentiated epithelial cells, multipotent 'basal cell-like' epithelial cells and inflammatory cells. 1×10^4 of these 'original' cells were plated on to rat-tail collagen I coated 24-well, 0.4 µm pore sized transparent PET (Polyethylene Terephthalate) membranes in the presence of 10 µM of Rho

Kinase inhibitor, Y-27,632 dihydrochloride (ROCKi, Tocris Bioscience). Cells were cultured to confluence in submerged culture and subsequently grown at the ALI for up to 7 days. Cells were lysed in 250 µl of Trizol reagent (Sigma-Aldrich) for RNA extraction at ALI day 0, day 3, and day 7. Fig. 1A gives a brief overview of the complete cell culture system.

RNA extraction and reverse transcription PCR (RT-PCR)
For end-point RT-PCR, total RNA was extracted from freshly isolated mMEECs before seeding (original) and cells at ALI days 0, 3 and 7 lysed in Trizol. RNA yield was determined using NanoDrop-1000 (Thermo Fisher Scientific). Residual genomic DNA was digested by DNase I treatment (Promega, cat. No-M6101) and 200 ng of RNA was reverse transcribed using AMV Reverse Transcriptase (Promega, cat. No-M9004). RT-PCR was performed with 1 µl of template cDNA and Maxima Hot Start Green PCR Master Mix (Thermo Fisher Scientific, cat. No-K1061). The cycling conditions were: 95°C for 5 min; denaturation: 94°C for 1 min (25–35 cycles); annealing: 60°C for 1 min; extension: 72°C for 1 min; final extension: 72°C for 7 min (MJ Research PTC-200). The primer pairs used are as follows: Bpifa1F, ACAGAGGAGCCGACGTCTAA; Bpifa1R, CCAAGAAAGCT-GAAGGTTC; Tekt1 F, CAGTGCGAAGTGGTAGACG; Tekt1R, TTCAC-CTGGATTTCCTCCTG; Oaz1F, ACAGAGGAGCCGACGTCTAA; Oaz1R, CCAAGAAAGCTGAAGGTTC; Spata18F, GCAATGCAGTCCTTAGAG-CC; Spata18R,CATTACTGGTCGCACGGAC; Dynlrb2F, CCACAGGCG-CGATGACAG; Dynlrb2R,ACTCACATGGGTTCTGAATGACA; Cdhr3F, AGGTGGAAAGGCCCATTAAC; Cdhr3R, AGTCGTAGAAGGGCATC-AGG. The amplified PCR products were run on a 2% agarose gel containing 0.5 µg/ml ethidium bromide and bands visualised using a Bio-Rad ChemiDoc™ XRS+.

Clariom S mouse microarray
Samples of total RNA (*n*=3 at each time point) were checked for quantity and quality using the Nanodrop and Agilent Bionalyser 600. Subsequently 200 ng was prepared for analysis on the Clariom S mouse GeneChip (Thermo Fisher Scientific) according to the manufacturers' instructions. Briefly mRNA was converted to double stranded cDNA with the incorporation of a T7 polymerase binding site at the 3′ end of the RNA molecule. Antisense RNA was generated by utilization of the T7 polymerase. This was purified using a magnetic bead process and further quantified on the Nanodrop. 15 ug of the aRNA was taken forward to generate a sense DNA strand. This was fragmented and end labelled with biotin before being incorporated into a hybridization solution and incubated with the GeneChip. Following post hybridisation washing using the fluidics station a fluorescent signal corresponding to hybridization of the labelled material to the oligonucleotide probes on the chip was achieved using a streptavidin-phycoerythrein cocktail. Gene chips were scanned on the Gene Chip 7000G scanner and the images collected as CEL files. Raw data from this study has been submitted to NCBI with the submission number GSE150764.

Bioinformatic analysis
Microarray data in CEL files was analysed using Affymetrix Expression Console. Gene level summary data were obtained using the RMA summarization method. Differentially expressed genes were identified using Limma (Smyth, 2004) with the criteria of absolute fold change>2 and Limma adjusted *P*-value<0.05. Batch effect was included in the statistical models. *P*-values were adjusted with the Benjamini and Hochberg method (Benjamini and Hochberg, 1995). A gene can have more than one probe sets. If a gene had both up- and downregulated probe sets, it was removed from the list of differentially expressed genes. Multidimensional scaling plot were generated using Limma. Gene ontology analyses were performed using clusterProfiler (Yu et al., 2012).

References
Allen, E. K., Chen, W. M., Weeks, D. E., Chen, F., Hou, X., Mattos, J. L., Mychaleckyj, J. C., Segade, F., Casselbrant, M. L., Mandel, E. M. et al. (2013). A genome-wide association study of chronic otitis media with effusion and recurrent otitis media identifies a novel susceptibility locus on chromosome 2. *J. Assoc. Res. Otolaryngol.* **14**, 791-800. doi:10.1007/s10162-013-0411-2

Azar, A., Piccinelli, C., Brown, H., Headon, D. and Cheeseman, M. (2016). Ectodysplasin signalling deficiency in mouse models of hypohidrotic ectodermal dysplasia leads to middle ear and nasal pathology. *Hum. Mol. Genet.* **25**, 3564-3577. doi:10.1093/hmg/ddw202

Bakaletz, L. O. (2010). Immunopathogenesis of polymicrobial otitis media. *J. Leukoc. Biol.* **87**, 213-222. doi:10.1189/jlb.0709518

Benjamini, Y. and Hochberg, Y. (1995). Controlling the false discovery rate: a practical and powerful approach to multiple testing. *J. R. Stat. Soc. B* **57**, 289-300. doi:10.1111/j.2517-6161.1995.tb02031.x

Bhaskaran, M., Chen, H., Chen, Z. and Liu, L. (2005). Hemoglobin is expressed in alveolar epithelial type II cells. *Biochem. Biophys. Res. Commun.* **333**, 1348-1352. doi:10.1016/j.bbrc.2005.06.042

Bhutta, M. F., Lambie, J., Hobson, L., Goel, A., Hafrén, L., Einarsdottir, E., Mattila, P. S., Farrall, M., Brown, S. D. and Burton, M. J. (2017). A mouse-to-man candidate gene study identifies association of chronic otitis media with the loci TGIF1 and FBXO11. *Sci. Rep.* **7**, 12496. doi:10.1038/s41598-017-12784-8

Biagioli, M., Pinto, M., Cesselli, D., Zaninello, M., Lazarevic, D., Roncaglia, P., Simone, R., Vlachouli, C., Plessy, C., Bertin, N. et al. (2009). Unexpected expression of alpha- and beta-globin in mesencephalic dopaminergic neurons and glial cells. *Proc. Natl. Acad. Sci. USA* **106**, 15454-15459. doi:10.1073/pnas.0813216106

Bornstein, C., Brosh, R., Molchadsky, A., Madar, S., Kogan-Sakin, I., Goldstein, I., Chakravarti, D., Flores, E. R., Goldfinger, N., Sarig, R. et al. (2011). SPATA18, a spermatogenesis-associated gene, is a novel transcriptional target of p53 and p63. *Mol. Cell. Biol.* **31**, 1679-1689. doi:10.1128/MCB.01072-10

Chen, Y., Val, S., Krueger, A., Zhong, L., Panigrahi, A., Nino, G., Wolf, S. and Preciado, D. (2019). Human primary middle ear epithelial cell culture: a novel in vitro model to study otitis media. *Laryngoscope Investig. Otolaryngol.* **4**, 663-672. doi:10.1002/lio2.319

Choksi, S. P., Lauter, G., Swoboda, P. and Roy, S. (2014). Switching on cilia: transcriptional networks regulating ciliogenesis. *Development* **141**, 1427-1441. doi:10.1242/dev.074666

Chu, Q., Yao, C., Qi, X., Stripp, B. R. and Tang, N. (2019). STK11 is required for the normal program of ciliated cell differentiation in airways. *Cell Discovery* **5**, 36. doi:10.1038/s41421-019-0104-z

Crompton, M., Purnell, T., Tyrer, H. E., Parker, A., Ball, G., Hardisty-Hughes, R. E., Gale, R., Williams, D., Dean, C. H., Simon, M. M. et al. (2017). A mutation in Nischarin causes otitis media via LIMK1 and NF-κB pathways. *PLoS Genet.* **13**, e1006969. doi:10.1371/journal.pgen.1006969

Cross, M., Mangelsdorf, I., Wedel, A. and Renkawitz, R. (1988). Mouse lysozyme M gene: isolation, characterization, and expression studies. *Proc. Natl. Acad. Sci. USA* **85**, 6232-6236. doi:10.1073/pnas.85.17.6232

Davidoss, N. H., Varsak, Y. K. and Santa Maria, P. L. (2018). Animal models of acute otitis media - A review with practical implications for laboratory research. *Eur Ann Otorhinolaryngol Head Neck Dis* **135**, 183-190. doi:10.1016/j.anorl.2017.06.013

Del-Pozo, J., MacIntyre, N., Azar, A., Glover, J., Milne, E. and Cheeseman, M. (2019). Chronic otitis media is initiated by a bulla cavitation defect in the FBXO11 mouse model. *Dis Model Mech* **12**, dmm038315.

Edfors, F., Danielsson, F., Hallström, B. M., Käll, L., Lundberg, E., Pontén, F., Forsström, B. and Uhlén, M. (2016). Gene-specific correlation of RNA and protein levels in human cells and tissues. *Mol. Syst. Biol.* **12**, 883. doi:10.15252/msb.20167144

Einarsdottir, E., Hafrén, L., Leinonen, E., Bhutta, M. F., Kentala, E., Kere, J. and Mattila, P. S. (2016). Genome-wide association analysis reveals variants on chromosome 19 that contribute to childhood risk of chronic otitis media with effusion. *Sci. Rep.* **6**, 3324. doi:10.1038/srep33240

Everman, J. L., Sajuthi, S., Saef, B., Rios, C., Stoner, A. M., Numata, M., Hu, D., Eng, C., Oh, S., Rodriguez-Santana, J. et al. (2019). Functional genomics of CDHR3 confirms its role in HRV-C infection and childhood asthma exacerbations. *J. Allergy Clin. Immunol.* **144**, 962-971. doi:10.1016/j.jaci.2019.01.052

Giese, A., Ali, S., Isaiah, A., Aziz, I., Riazuddin, S. and Ahmed, Z. M. (2020). Genomics of Otitis Media (OM): Molecular Genetics Approaches to Characterize Disease Pathophysiology. *Front. Genet.* **11**, 313. doi:10.3389/fgene.2020.00313

Hardisty-Hughes, R. E., Tateossian, H., Morse, S. A., Romero, M. R., Middleton, A., Tymowska-Lalanne, Z., Hunter, A. J., Cheeseman, M. and Brown, S. D. (2006). A mutation in the F-box gene, Fbxo11, causes otitis media in the Jeff mouse. *Hum. Mol. Genet.* **15**, 3273-3279. doi:10.1093/hmg/ddl403

Hernandez, M., Leichtle, A., Pak, K., Webster, N. J., Wasserman, S. I. and Ryan, A. F. (2015). The transcriptome of a complete episode of acute otitis media. *BMC Genomics* **16**, 259. doi:10.1186/s12864-015-1475-7

Juhn, S. K., Jung, M. K., Hoffman, M. D., Drew, B. R., Preciado, D. A., Sausen, N. J., Jung, T. T., Kim, B. H., Park, S. Y., Lin, J. et al. (2008). The role of inflammatory mediators in the pathogenesis of otitis media and sequelae. *Clinical and Experimental Otorhinolaryngology* **1**, 117-138. doi:10.3342/ceo.2008.1.3.117

Kerschner, J. E., Hong, W., Taylor, S. R., Kerschner, J. A., Khampang, P., Wrege, K. C. and North, P. E. (2013). A novel model of spontaneous otitis media with effusion (OME) in the Oxgr1 knock-out mouse. *Int. J. Pediatr. Otorhinolaryngol.* **77**, 79-84. doi:10.1016/j.ijporl.2012.09.037

Kurabi, A., Pak, K., Ryan, A. F. and Wasserman, S. I. (2016). Innate immunity: orchestrating inflammation and resolution of otitis media. *Curr. Allergy Asthma Rep.* **16**, 6. doi:10.1007/s11882-015-0585-2

Luo, W., Yi, H., Taylor, J., Li, J. D., Chi, F., Todd, N. W., Lin, X., Ren, D. and Chen, P. (2017). Cilia distribution and polarity in the epithelial lining of the mouse middle ear cavity. *Sci. Rep.* **7**, 45870. doi:10.1038/srep45870

MacArthur, C. J., Hefeneider, S. H., Kempton, J. B. and Trune, D. R. (2006). C3H/HeJ mouse model for spontaneous chronic otitis media. *Laryngoscope* **116**, 1071-1079. doi:10.1097/01.mlg.0000224527.41288.c4

MacArthur, C. J., Hausman, F., Kempton, J. B., Choi, D. and Trune, D. R. (2013). Otitis media impacts hundreds of mouse middle and inner ear genes. *PloS one* **8**, e75213. doi:10.1371/journal.pone.0075213

Mata, M., Milian, L., Armengot, M. and Carda, C. (2014). Gene mutations in primary ciliary dyskinesia related to otitis media. *Curr. Allergy Asthma Rep.* **14**, 420. doi:10.1007/s11882-014-0420-1

Monasta, L., Ronfani, L., Marchetti, F., Montico, M., Vecchi Brumatti, L., Bavcar, A., Grasso, D., Barbiero, C. and Tamburlini, G. (2012). Burden of disease caused by otitis media: systematic review and global estimates. *PLoS ONE* **7**, e36226. doi:10.1371/journal.pone.0036226

Montoro, D. T., Haber, A. L., Biton, M., Vinarsky, V., Lin, B., Birket, S. E., Yuan, F., Chen, S., Leung, H. M., Villoria, J. et al. (2018). A revised airway epithelial hierarchy includes CFTR-expressing ionocytes. *Nature* **560**, 319-324. doi:10.1038/s41586-018-0393-7

Mulay, A., Akram, K. M., Williams, D., Armes, H., Russell, C., Hood, D., Armstrong, S., Stewart, J. P., Brown, S. D., Bingle, L. et al. (2016). An in vitro model of murine middle ear epithelium. *Dis Model Mech* **9**, 1405-1417. doi:10.1242/dmm.026658

Mulay, A., Hood, D. W., Williams, D., Russell, C., Brown, S. D. M., Bingle, L., Cheeseman, M. and Bingle, C. D. (2018). Loss of the homeostatic protein BPIFA1, leads to exacerbation of otitis media severity in the Junbo mouse model. *Sci. Rep.* **8**, 3128. doi:10.1038/s41598-018-21166-7

Mulay, A., Akram, K., Bingle, L. and Bingle, C. D. (2019). Isolation and culture of primary mouse middle ear epithelial cells. *Methods Mol. Biol.* **1940**, 157-168. doi:10.1007/978-1-4939-9086-3_11

Musa, M., Wilson, K., Sun, L., Mulay, A., Bingle, L., Marriott, H. M., LeClair, E. E. and Bingle, C. D. (2012). Differential localisation of BPIFA1 (SPLUNC1) and BPIFB1 (LPLUNC1) in the nasal and oral cavities of mice. *Cell Tissue Res.* **350**, 455-464. doi:10.1007/s00441-012-1490-9

Noben-Trauth, K. and Latoche, J. R. (2011). Ectopic mineralization in the middle ear and chronic otitis media with effusion caused by RPL38 deficiency in the Tail-short (Ts) mouse. *J. Biol. Chem.* **286**, 3079-3093. doi:10.1074/jbc.M110.184598

Parkinson, N., Hardisty-Hughes, R. E., Tateossian, H., Tsai, H. T., Brooker, D., Morse, S., Lalane, Z., MacKenzie, F., Fray, M., Glenister, P. et al. (2006). Mutation at the Evi1 locus in Junbo mice causes susceptibility to otitis media. PLoS Genet. 2, e149. doi:10.1371/journal.pgen.0020149

Phipson, B., Lee, S., Majewski, I. J., Alexander, W. S. and Smyth, G. K. (2016). Robust hyperparameter estimation protects against hypervariable genes and improves power to detect differential expression. Ann Appl Stat 10, 946-963. doi:10.1214/16-AOAS920

Preciado, D., Goyal, S., Rahimi, M., Watson, A. M., Brown, K. J., Hathout, Y. and Rose, M. C. (2010). MUC5B Is the predominant mucin glycoprotein in chronic otitis media fluid. Pediatr. Res. 68, 231-236. doi:10.1203/PDR.0b013e3181eb2ecc

Preciado, D., Burgett, K., Ghimbovschi, S. and Rose, M. C. (2013). NTHi Induction of Cxcl2 and middle ear mucosal metaplasia in mice. Laryngoscope 123, E66-E71. doi:10.1002/lary.24097

Roy, M. G., Livraghi-Butrico, A., Fletcher, A. A., McElwee, M. M., Evans, S. E., Boerner, R. M., Alexander, S. N., Bellinghausen, L. K., Song, A. S., Petrova, Y. M. et al. (2014). Muc5b is required for airway defence. Nature 505, 412-416. doi:10.1038/nature12807

Ryan, A. F., Nasamran, C. A., Pak, K., Draf, C., Fisch, K. M., Webster, N. and Kurabi, A. (2020). Single-Cell Transcriptomes Reveal a Complex Cellular Landscape in the Middle Ear and Differential Capacities for Acute Response to Infection. Frontiers in genetics 11, 358. doi:10.3389/fgene.2020.00358

Rye, M. S., Bhutta, M. F., Cheeseman, M. T., Burgner, D., Blackwell, J. M., Brown, S. D. and Jamieson, S. E. (2011). Unraveling the genetics of otitis media: from mouse to human and back again. Mamm. Genome 22, 66-82. doi:10.1007/s00335-010-9295-1

Rye, M. S., Warrington, N. M., Scaman, E. S. H., Vijayasekaran, S., Coates, H. L., Anderson, D., Pennell, C. E., Blackwell, J. M. and Jamieson, S. E. (2012). Genome-wide association study to identify the genetic determinants of otitis media susceptibility in childhood. Plos One 7, e48215. doi:10.1371/journal.pone.0048215

Santos-Cortez, R. L., Chiong, C. M., Reyes-Quintos, M. R., Tantoco, M. L., Wang, X., Acharya, A., Abbe, I., Giese, A. P., Smith, J. D., Allen, E. K. et al. (2015). Rare A2ML1 variants confer susceptibility to otitis media. Nat. Genet. 47, 917-920. doi:10.1038/ng.3347

Santos-Cortez, R. L. P., Chiong, C. M., Frank, D. N., Ryan, A. F., Giese, A. P. J., Bootpetch Roberts, T., Daly, K. A., Steritz, M. J., Szeremeta, W., Pedro, M. et al. (2018). FUT2 Variants Confer Susceptibility to Familial Otitis Media. Am. J. Hum. Genet. 103, 679-690. doi:10.1016/j.ajhg.2018.09.010

Smyth, G. K. (2004). Linear models and empirical bayes methods for assessing differential expression in microarray experiments. Stat. Appl. Genet. Mol. Biol. 3, Article3. doi:10.2202/1544-6115.1027

Stamatoyannopoulos, G. (2005). Control of globin gene expression during development and erythroid differentiation. Exp. Hematol. 33, 259-271. doi:10.1016/j.exphem.2004.11.007

Tateossian, H., Morse, S., Parker, A., Mburu, P., Warr, N., Acevedo-Arozena, A., Cheeseman, M., Wells, S. and Brown, S. D. (2013). Otitis media in the Tgif knockout mouse implicates TGFβ signalling in chronic middle ear inflammatory disease. Hum. Mol. Genet. 22, 2553-2565. doi:10.1093/hmg/ddt103

Thompson, H. and Tucker, A. S. (2013). Dual Origin of the Epithelium of the Mammalian Middle Ear. Science 339, 1453-1456. doi:10.1126/science.1232862

Tucker, A. S., Dyer, C. J., Fons Romero, J. M., Teshima, T. H. N., Fuchs, J. C. and Thompson, H. (2018). Mapping the distribution of stem/progenitor cells across the mouse middle ear during homeostasis and inflammation. Development 145, dev154393. doi:10.1242/dev.154393

van Ingen, G., Li, J., Goedegebure, A., Pandey, R., Li, Y. R., March, M. E., Jaddoe, V. W., Bakay, M., Mentch, F. D., Thomas, K. et al. (2016). Genome-wide association study for acute otitis media in children identifies FNDC1 as disease contributing gene. Nat. Commun. 7, 12792. doi:10.1038/ncomms12792

Woodfield, G. and Dugdale, A. (2008). Evidence behind the WHO guidelines: hospital care for children: what is the most effective antibiotic regime for chronic suppurative otitis media in children. J. Trop. Pediatr. 54, 151-156. doi:10.1093/tropej/fmn042

Yu, G., Wang, L. G., Han, Y. and He, Q. Y. (2012). clusterProfiler: an R package for comparing biological themes among gene clusters. OMICS 16, 284-287. doi:10.1089/omi.2011.0118

Ziegler, C., Allon, S. J., Nyquist, S. K., Mbano, I. M., Miao, V. N., Tzouanas, C. N., Cao, Y., Yousif, A. S., Bals, J., Hauser, B. M. et al. (2020). SARS-CoV-2 Receptor ACE2 is an interferon-stimulated gene in human airway epithelial cells and is detected in specific cell subsets across tissues. Cell 181, 1016-1035. doi:10.1016/j.cell.2020.04.035

Table S1. Differential gene expression of MEECs Day 0 vs original

Click here to download Table S1

Table S2. Differential gene expression of MEECs Day 7 vs Day 0

Click here to download Table S2

Table S3. Differential gene expression of MEECs Day 7 vs original

Click here to download Table S3